Published in final edited form as:
Immunity. 2009 August 21; 31(2): 245–258. doi:10.1016/j.immuni.2009.06.018.

Apoptotic cells promote their own clearance and immune tolerance through activation of LXR

Noelia A-Gonzalez[1], **Steven J. Bensinger**[2,3], **Cynthia Hong**[2,3], **Susana Beceiro**[1], **Michelle N. Bradley**[2,3], **Noam Zelcer**[2,3], **Jose Deniz**[1], **Cristina Ramirez**[1], **Merci Díaz**[1], **German Gallardo**[1], **Carlos Ruiz de Galarreta**[1], **Jon Salazar**[2,3], **Felix Lopez**[1], **Peter Edwards**[4], **John Parks**[5], **Miguel Andujar**[6], **Peter Tontonoz**[2,3,*], and **Antonio Castrillo**[1,7,*]

[1]Immune Signaling Laboratory, Department of Biochemistry and Molecular Biology; School of Medicine, University of Las Palmas, ULPGC. Las Palmas, 35016, Spain

[2]Howard Hughes Medical Institute, University of California, Los Angeles, California 90095, USA

[3]Department of Pathology and Laboratory Medicine, University of California, Los Angeles, California 90095, USA

[4]Department of Biological Chemistry, University of California, Los Angeles, California 90095, USA

[5]Department of Pathology, Wake Forest University School of Medicine, Winston- Salem, NC 27157, USA

[6]Pathology Dept., Hospital Universitario Materno-Infantil. Las Palmas, 35016, Spain

[7]Instituto de Investigaciones Biomédicas Alberto Sols. 28029 Madrid. Consejo Superior de Investigaciones Científicas. CSIC. Spain

Summary

Effective clearance of apoptotic cells by macrophages is essential for immune homeostasis. The transcriptional pathways that allow macrophages to sense and respond to apoptotic cells are poorly defined. We demonstrate here that LXR signaling is important for both apoptotic cell clearance and the maintenance of immune tolerance. Apoptotic cell engulfment activates LXR and thereby induces the expression of Mer, a receptor tyrosine kinase critical for phagocytosis. LXR null macrophages exhibit a selective defect in phagocytosis of apoptotic cells and an aberrant pro-inflammatory response to them. As a consequence of these defects, mice lacking LXRs manifest a breakdown in self-tolerance and develop autoantibodies and autoimmune glomerulonephritis. Treatment with an LXR agonist ameliorates disease progression in mouse models of Lupus-like autoimmunity. Thus, activation of LXR by apoptotic cells engages a virtuous cycle that promotes their own clearance and couples engulfment to the suppression of inflammatory pathways.

*Corresponding Authors: Peter Tontonoz M.D., Ph.D., Howard Hughes Medical Institute, UCLA School of Medicine, Box 951662, Los Angeles, CA 90095-1662, Phone: (310) 206-4546, ptontonoz@mednet.ucla.edu; Antonio Castrillo, Ph.D., Instituto Investigaciones Biomedicas Alberto Sols, Consejo Superior de Investigaciones Científicas, CSIC and Department of Biochemistry and Molecular Biology, University of Las Palmas, 35016. Spain. Phone: (34) 928-459681, acastrillo@iib.uam.es
Current address: Institute for Molecular Medicine, Department of Pathology and Laboratory Medicine, University of California, Los Angeles 90095

Introduction

Apoptosis occurs through a series of controlled events that ensure cellular remnants are contained and eliminated without initiating an inflammatory immune response (Grimsley and Ravichandran, 2003; Henson et al., 2001; Savill and Fadok, 2000). In general, apoptotic cell sensing systems recognize lipid or carbohydrate changes displayed on the outside of the dying cell, such as phosphatidylserine (PtdSer), a membrane lipid normally restricted to the inner leaflet of the plasma membrane (Green, 2003; Ravichandran and Lorenz, 2007). The loss of membrane asymmetry during apoptosis also leads to oxidation of phospholipids. These so called "eat-me" signals are bound by bridging molecules including milk fat globule EGF factor 8 (MFGE8), growth-arrest-specific 6 (GAS6) and complement factor C1q on the surface of apoptotic cells (Botto et al., 1998; Hanayama et al., 2002; Ishimoto et al., 2000). Bridging molecules facilitate phagocytosis through interaction with specific receptors expressed on macrophages and dendritic cells, including the TAM family of receptors (Tyro3, Axl, and Mer), $\alpha_v\beta_3$-integrin, Tim4 and CD36 (Fadok et al., 1998; Lemke and Rothlin, 2008; Miyanishi et al., 2007; Ravichandran and Lorenz, 2007).

Following apoptotic cell engulfment, macrophages activate tolerogenic pathways in an effort to prevent immune responses against self antigens (Henson and Hume, 2006; Taylor et al., 2005). Tolerance is accomplished through several distinct mechanisms, including suppression of inflammatory cytokine production and release of anti-inflammatory cytokines such as IL-10 and TGF-β (Fadok et al., 1998; Li and Flavell, 2008; Voll et al., 1997). If phagocytosis or tolerogenic pathways are impaired, chronic accumulation of free apoptotic material can have pathological consequences (Henson and Hume, 2006; O'Shea et al., 2002). The resulting inflammation and stimulation of adaptive immune responses against self-antigens may ultimately trigger autoimmunity (Ravichandran and Lorenz, 2007; Savill et al., 2002). Interestingly, TAM receptors have recently been linked to the suppression of TLR signaling, revealing one mechanism by which apoptotic cell clearance and immune tolerance are coupled (Lemke and Rothlin, 2008; Rothlin et al., 2007). Transcriptional pathways integrating apoptotic cell clearance and the immunosuppressive effects of apoptotic cells remain to be characterized.

Liver X Receptors (LXRα and LXRβ) are oxysterol-activated transcription factors that sense elevated levels of cellular cholesterol (Peet et al., 1998; Repa and Mangelsdorf, 2002). Accumulation of excess lipoprotein-derived cholesterol in macrophages activates LXR and triggers the induction of a transcriptional program for cholesterol efflux (Castrillo and Tontonoz, 2004). Pharmacologically activated LXRs have also been shown to transrepress inflammatory gene expression (Castrillo et al., 2003a; Ghisletti et al., 2007; Joseph et al., 2003). However, the physiological relevance of endogenous transrepression pathways has remained unclear, since no biological processes have been definitively shown to be dependent on both activation and transrepression. We reasoned that the dual abilities of LXRs to respond to phagocytosed lipids and to modulate inflammation places them in an ideal position to tailor macrophage responses to particular phagocytic contexts. We demonstrate here that the LXR pathway is essential for efficient apoptotic cell clearance through positive gene induction of Mer, as well as for the maintenance of immune tolerance through transrepression of inflammation in response to phagocytosis. These results implicate LXRs in a positive transcriptional feedback loop that couples apoptotic cell clearance with the suppression of autoimmunity.

Results

Defective phagocytosis of apoptotic cells in *Lxrαβ-/-* macrophages

Previous work has established that LXRα and LXRβ are important for the macrophage response to lipoprotein uptake (Castrillo and Tontonoz, 2004), but their impact on other phagocytic

processes is unknown. To investigate a possible role of LXRs in apoptotic cell clearance, thioglycollate-elicited macrophages obtained from WT and *Lxr*αβ-/- mice were co-cultured *in vitro* with apoptotic thymocytes (AT). Engulfed AT were differentiated from associated AT through use of a cell dissociation buffer (Krysko et al., 2006), and by scoring engulfed cells by confocal microscopy (Fig. 1A,B). We found that AT were efficiently engulfed by WT macrophages, whereas phagocytosis by *Lxr*αβ-/- macrophages was markedly reduced. By contrast, phagocytosis of GFP-*E.Coli* or fluorescent microspheres was comparable in WT and *Lxr*αβ-/- macrophages, indicating that loss of LXR function does not lead to a general defect in phagocytosis (Fig. S1). To determine if apoptotic cell clearance could be improved by exogenous stimulation of LXR activity, macrophages were cultured with the synthetic LXR agonist GW3965 (Collins et al., 2002) for 48 h and then challenged with apoptotic cells for 1 h. GW3965 enhanced WT macrophage phagocytosis, but had no effect in macrophages lacking LXRs (Fig. 1C,D).

These LXR-dependent mechanisms also appear to function *in vivo*. Resident macrophages of *Lxr*αβ-/- mice exhibited reduced AT association (combination of bound and engulfed cells) in response to intraperitoneal injection of cfse-labeled AT compared to macrophages of C57BL/6 mice (Fig. 1E). Furthermore, primary macrophages from mice treated with GW3965 for 3 days displayed increased AT association compared to vehicle treated mice (Fig. S2). AT association in this assay was specific for macrophages, because we observed no association of AT with peritoneal B cells (Fig. S3A). Furthermore, defective AT association of *Lxr*αβ-/- macrophages could not be attributed to loss of regulation of the established LXR targets *Abca1*, *Abcg1* or *ApoE*, because mice lacking expression of these genes showed comparable AT association to WT cells (Fig. S3B,C). Note, *Abca1* null mice on a C57Bl/6 background are not viable and therefore comparison was made to background-matched *Abca1*+/+ controls (Fig. S4C). LXR-dependent regulation of AT phagocytosis was also observed in both immature and mature dendritic cells (Fig. S3D).

Altered macrophage functions in *Lxr*αβ-/- lymphoid tissues

Next we investigated the potential consequences of loss of LXR function for apoptotic cell clearance *in vivo.* Immunofluorescence analysis of *Lxr*αβ-/- spleens showed increased numbers of germinal centers staining with peanut agglutinin (PNA) and increased numbers of immunoglobulin G (IgG)-producing cells (Fig. 2A). In addition, *Lxr*αβ-/- spleens showed an anomalous distribution of CD68+F4/80- “tingible body” macrophages (Rabinowitz and Gordon, 1991) (Fig. 2A). Staining of endothelial sinus-lining cells with MadCAM-1 also demonstrated defects in the organization of the spleen in older *Lxr*αβ-/- mice (Fig.2A). Macrophages present in germinal centers participate in the clearance of apoptotic B cells (Smith et al., 1991;Taylor et al., 2005). Accordingly, few apoptotic cells were typically observed in the spleens of WT mice, and these co-localized with macrophages (Fig. 2B, left panel). In contrast, despite comparable numbers of splenic CD68+ macrophages (data not shown), many free apoptotic bodies were present in *Lxr*αβ-/- spleens, consistent with inefficient macrophage engulfment (Fig. 2B, right panel). Free apoptotic bodies were also observed in several other tissues of *Lxr*αβ-/- mice, including thymus, lung and testis (Fig. S4A). We have previously reported that macrophages lacking LXR expression undergo apoptosis when challenged with Listeria monocytogenes (Joseph et al., 2004). However, *Lxr*αβ-/- macrophages do not undergo apoptosis at an increased rate compared to WT when challenged with AT. The apoptotic bodies observed in *Lxr*αβ-/- spleens colocalized with B cells (Fig. S4B), but not with macrophages (Fig. 2B). Furthermore, *Lxr*αβ-/- macrophages challenged with AT *in vitro* for extended times (18 h) do not undergo apoptosis as assayed by TUNEL staining (Fig. S4C,D and data not shown).

We also evaluated the clearance of dying thymocytes following dexamethasone (dex) induced apoptosis *in vivo*. Both WT and *Lxr*αβ-/- thymocytes showed comparable sensitivity to dex- or UV irradiation-induced apoptosis *in vitro* (Fig. S5). After 24 h of dex stimulation, thymi of WT mice showed a marked loss of mass and few Annexin V+ cells, consistent with effective clearance of apoptotic cells (Fig. 2C,D). By contrast, despite similar recruitment of CD68+ macrophages, *Lxr*αβ-/- thymi contained increased numbers of free Annexin V+ cells and mass was not significantly altered. In agreement with these results, transmission electron microscopy analysis of thymic sections revealed effective engulfment of apoptotic bodies by WT macrophages (Fig. 2E; see inset, a macrophage with 5 apoptotic cells inside), whereas abundant clusters of free apoptotic cells (large dark staining bodies) were observed in *Lxr*αβ-/- mice (Fig. 2E). Thus, loss of LXR function results in defective clearance of apoptotic cells *in vivo*.

Transcriptional regulation of genes involved in clearance of apoptotic cells by LXRs

To identify LXR target genes involved in the removal of apoptotic cells, we conducted transcriptional profiling studies using RAW264.7 cells ectopically expressing LXRα (Venkateswaran et al., 2000) (RAW-LXRα; Fig. S6A). These studies identified the gene encoding the Mer receptor tyrosine kinase (Camenisch et al., 1999; Graham et al., 1995) as a novel LXR-responsive gene (Fig. S6B). Mer plays an important role in the clearance of dying cells through interaction with PtdSer-bound Gas6 on the surface of apoptotic cells (Cohen et al., 2002; Lemke and Rothlin, 2008; Scott et al., 2001). Realtime PCR and Western analysis of RAW-LXRα cells and primary macrophages confirmed that *Mer* was a *bona fide* LXR-responsive gene (Fig. 3A,B,C). Expression of *Mer* was induced by LXR and RXR agonists in WT, *Lxr*α-/- and *Lxr*β-/- but not in *Lxr*αβ-/- primary macrophages (Fig. 3C and S6B), indicating that *Mer* responds to both LXRα and LXRβ. Expression of the other members of the TAM family, *Tyro3* and *Axl*, was not altered by LXR agonists (Fig. S6A and data not shown). Although several different RXR heterodimeric nuclear receptors are expressed in macrophages, the effect of RXR agonists on Mer expression was absolutely dependent on LXR expression (Fig. 3B,C).

Importantly, Mer expression was also responsive to LXR activation *in vivo.* Treatment for 3 days with GW3965 induced expression of Mer in spleen and lung of WT but not *Lxr*αβ-/- mice (Fig 3D). Basal expression of Mer mRNA was also impaired in primary cells and lymphoid organs of *Lxr*αβ-/- mice (Fig. 3C,D and not shown). To determine if the Mer gene was a direct target for LXRs, we analyzed the 5′-promoter region. A potential LXRE (LXR response element) was identified 1.7 kb upstream of the transcription start site (Fig. S7A). Electromobility shift assays demonstrated that *in vitro* translated LXR and RXR proteins bound as heterodimers to a radiolabeled oligonucleotide containing this element (Fig. S7A). Binding of LXR to the Mer promoter was also confirmed by chromatin immunoprecipitation (ChIP) analysis of RAW-FLAG-LXRα cells (Fig. S7B). ChIP assays using either anti-FLAG or anti-RXRα antibodies demonstrated the presence of LXR/RXR heterodimers on the Mer promoter. Furthermore, GW3965 caused release of N-CoR from and recruitment of RNA polymerase II to both the Mer and SREBP-1c promoters in RAW-LXRα cells (Fig. S7C).

Ingestion and degradation of apoptotic cells by macrophages leads to the accumulation of cellular components, including cholesterol. We hypothesized that such accumulation might activate LXR signaling. Remarkably, expression of *Mer* and a battery of known LXR targets (*Abca1*, *Abcg5*, *Pltp*, and *Glut4*), was induced by apoptotic thymocytes (AT) in WT macrophages (Fig. 3A). By contrast, induction of these genes by AT was severely impaired *Lxr*αβ-/- macrophages. Some residual induction of *Mer* by AT remained in *Lxr*αβ-/- macrophages, pointing to the contribution of an additional, LXR-independent pathway. Genes not regulated by LXR, such as and CD36, were induced by AT to comparable levels in both WT and *Lxr*αβ-/- macrophages (Fig. 3A). Expression of Mfge8 was not responsive to AT or

LXR signaling. Thus, LXR mediates the AT-dependent regulation of a specific subset of genes involved in phagocytosis and lipid metabolism. These results suggest that engulfment of apoptotic cells leads to activation of LXRs and the promotion of Mer expression, providing positive feedback to facilitate further apoptotic cell uptake. In support of this idea, we found that macrophages challenged with one round of AT show increased phagocytic capacity when challenged with a second round, and that this response was dependent on LXR expression (Fig. 3E). Furthermore, depletion of sterols from AT by means of methyl beta-cyclodextran treatment reduced their ability to induce LXR target gene expression (*Mer*, *Abca1*) following ingestion by macrophages, but not their ability to induce *Marco* or *cd36* expression. These results strongly suggest that cholesterol and/or oxysterol species present in AT can serve as LXR agonists (Fig. 3F). In support of this idea, Lauber et al reported that lipid mediators derived from apoptotic cells are important for efficient engulfment of dying corpses (Lauber et al., 2003).

Pro-inflammatory signaling in response to apoptotic cells in LXR null mice

Engulfment of apoptotic cells is coupled to the suppression of inflammatory pathways in order to avoid unwanted immune responses against intracellular antigens. Interestingly, both Mer and LXR have previously been implicated in the repression of macrophage inflammatory signaling (Camenisch et al., 1999; Joseph et al., 2003; Rothlin et al., 2007). Based on the abnormal phagocytic response of *Lxr*αβ-/- mice to apoptotic cells, we predicted that regulation of inflammatory pathways during the engulfment process might be also altered in *Lxr*αβ-/- macrophages. We therefore tested the ability of apoptotic cells to engage anti-inflammatory mechanisms in the presence or absence of LXR. In agreement with previous studies (Fadok et al., 1998; Voll et al., 1997), AT promoted the expression of immunosuppressive mediators such as *Tgf*-β and *Il-10* in WT macrophages (Fig. 4A,B). However, induction of these genes was impaired in macrophages lacking LXRs. Furthermore, inadequate engulfment of apoptotic cells by *Lxr*αβ-/- macrophages led to the inappropriate expression of pro-inflammatory mediators, such as IL-1β and MCP-1, and enhanced induction of Marco (Fig. 4A,B). LXR agonist alone repressed basal expression of IL-1β and MCP-1, but did not induce expression of *Tgf*-β and *Il-10* (Fig. S8A and data not shown).

We also tested the ability of apoptotic cells to counteract inflammatory signaling induced by ligands for toll-like receptors (TLR) 2, 3 and 4 (Fig. 4C and S8B). Culturing primary WT macrophages with AT inhibited the stimulus-dependent induction of IL-12p40 and IL-1β, in agreement with previous work (Fadok et al., 1998;Voll et al., 1997). By contrast, incubation of apoptotic thymocytes with *Lxr*αβ-/- macrophages resulted only in partial repression of inflammatory gene expression induced by LPS and other TLR activators (Fig. 4C and S8B). Thus LXR signaling couples the engulfment of apoptotic cells to the suppression of inflammatory pathways.

LXR-dependent expression of Mer promotes apoptotic cell clearance in macrophages

To further evaluate the role of Mer in LXR-dependent responses to apoptotic cells, we performed gain-of-function experiments. Retroviral expression of LXRα in RAW264.7 cells promoted the engulfment of AT in response to GW3965 (Fig. 5A,B). Ectopic expression of Mer itself also enhanced the phagocytosis of apoptotic cells, but this effect was not significantly modified by the addition of GW3965 (Fig. 5A,B). Treatment of WT macrophages with a Mer-blocking antibody (Sen et al., 2007) decreased AT phagocytosis to a similar level to that observed in LXR-deficient macrophages (Fig. 5C). To provide direct evidence for a link between LXR activation, Mer, and phagocytosis, we performed knockdown studies. RAW-LXRα cells were transfected with non-specific or several different Mer-specific siRNAs (Fig. 5D) and assayed for phagocytic activity. Reduction of Mer expression inhibited phagocytosis induced by LXR ligand, whereas non-specific siRNA had no effect (Fig. 5E). To further

confirm the role of the LXR-Mer pathway we performed knockdown studies in primary macrophages. Protein knockdown was verified by Western blotting (Fig. 5F). Reduction in Mer expression effectively inhibited the effect of LXR agonist on AT uptake, whereas knockdown of ABCA1 and apoE did not (Fig. 5G). These data show that LXR signaling promotes the clearance of apoptotic cells, at least in part, through induction of Mer expression.

*Lxr*αβ-/- mice develop age-dependent systemic autoimmune disease

Finally, we hypothesized that improper regulation of Mer expression and defective clearance of apoptotic cells would have pathological consequences for mice lacking LXRs. Analysis of lymphoid tissues from *Lxr*αβ-/- mice revealed age-dependent splenomegaly (Tangirala et al., 2002), lymphadenopathy and increased total cell numbers in these organs (Figs. 6A,B,C). A marked increase in the frequency and absolute numbers of CD19+B220+ B cells was observed in spleens and lymph nodes of *Lxr*αβ-/- mice (Fig. S9 and S10). The massive lymphadenopathy observed in older *Lxr*αβ-/- mice is reminiscent of the $MRL^{lpr/lpr}$ phenotype. However, we did not observe the accumulation of CD3+B220+DN T cells characteristic of $MRL^{lpr/lpr}$ mice in *Lxr*αβ-/- mice (Fig. S11). Furthermore, lymphoproliferative disease in *Lxr*αβ-/- mice did not appear to be a consequence of the loss of CD4+CD25+FoxP3+ regulatory T cells (Fig. S11). Defects in Mer signaling have previously been reported to result in the loss of self-tolerance and lupus-like disease (Cohen et al., 2002; Scott et al., 2001). Accordingly, elevated levels of antibodies to nuclear proteins (ANA, antinuclear antibodies), double-stranded DNA (dsDNA), and histones were detected in the serum of LXRαβ-/- mice (Fig. 6D).

A major pathogenic consequence of autoantibody production is the deposition of immune complexes in the kidney, leading to glomerulonephritis. Examination of kidney sections from WT and *Lxr*αβ-/- mice revealed conserved renal architecture in both genotypes (Fig. 6E and data not shown). However, *Lxr*αβ-/- mice exhibited glomerular enlargement, mesangial proliferation and glomerular basement membrane thickening (Fig. 6E). Immunofluorescence microscopy revealed marked age-dependent glomerular deposition of IgG-containing immune complexes and an inflammatory infiltrate of macrophages, B cells and T cells in kidneys of *Lxr*αβ-/- but not WT mice (Fig. 6F,G,H) and Fig. S12A**).** This observation is consistent with the development of age-dependent autoimmune disease due to autoantibody production. Moreover, the pathological changes in *Lxr*αβ-/- mice were associated with compromised renal function. Alterations in diuresis and urea excretion as well as markedly increased urinary protein concentrations were observed in a majority of 40-week old *Lxr*αβ-/- mice (Table S1). We also observed immunoglobulin deposition in multiple other tissues including lung and skin of *Lxr*αβ-/- mice, consistent with systemic autoimmune disease (Fig. S12B,C).

Full manifestation of the autoimmune phenotype required the combined deletion of both LXRα and LXRβ, consistent with the idea that macrophages (which express both LXRs) rather than lymphocytes (which only express LXRβ) are the primary cause of this pathology (Fig. S13A). Accordingly, the dramatic lymphoid hyperplasia and marked defects in apoptotic cell uptake and repression of inflammatory gene expression were observed only in mice and cells lacking both LXRα and LXRβ (data not shown). The autoimmune phenotype of *Lxr*αβ-/- mice is highly reminiscent of that of *Mer*-/- mice (Cohen et al., 2002). By contrast, similar disease was not observed in background-matched mice lacking the previously described LXR target genes *ApoE* and *Abcg1* (Fig. S12B). We also did not observe an increase in immunoglobulin deposition in *Abca1*-/- mice compared to background-matched controls (Fig. S13B).

LXR activation ameliorates lupus-like autoimmune disease in mice

Finally, we investigated whether pharmacological activation of LXR altered the development of autoimmune disease. Macrophages derived from $B6^{lpr/lpr}$ mice exhibited reduced phagocytic capacity compared to controls, consistent with prior work (Licht et al., 2004; Potter et al.,

2003; Qian et al., 2006). Remarkably, treatment of $B6^{lpr/lpr}$ macrophages with LXR agonist restored both phagocytic capacity and Mer expression to above basal control levels (Fig. 7A,B). To determine whether systemic administration of LXR agonist could ameliorate autoimmune disease, female $B6^{lpr/lpr}$ mice were treated for 4 months with GW3965. Strikingly, PET/CT imaging revealed a marked decrease in lymphadenopathy in GW3965 treated animals (Fig. 7C). Visual inspection of the lymph nodes confirmed the PET/CT images, and cell counts revealed an approximately 10-fold decrease in total cellularity (Fig. 7D). FACS analysis did not reveal any substantial differences in the frequency of specific immune cells in LN and spleen (data not shown). Although the extent of renal disease is mild on the B6 background, LXR nevertheless substantially reduced glomerular antibody deposition in $B6^{lpr/lpr}$ mice (Fig. 7E). Collectively, these results indicate that an intact LXR signaling pathway is important for Mer expression, apoptotic cell clearance and the maintenance of immune tolerance, and that pharmacologic activation of LXR antagonizes the pathogenesis of autoimmune disease.

Discussion

The balance between cell death and cell survival is crucial for tissue homeostasis in multicellular organisms (Green, 2003). Unwanted cells are usually eliminated by apoptosis, a programmed cellular suicide conserved from worms to mammals that culminates in recognition and ingestion of dying cells by phagocytes (Henson and Hume, 2006; Ravichandran and Lorenz, 2007). In contrast to other types of phagocytosis, such as bacterial or necrotic cell uptake, scavenging of apoptotic cells is immunologically silent (Lauber et al., 2004). Efficient disposal of apoptotic corpses prevents uncontrolled release of intracellular contents and is important for immunological self-tolerance (Ravichandran and Lorenz, 2007). Intracellular pathways that link the engulfment of apoptotic corpses and suppression of inflammation are incompletely characterized. We have shown here that the nuclear receptor LXR is important for both apoptotic cell clearance and suppression of the inflammatory response during their phagocytosis.

Prior work has shown LXR to be critical for macrophage cholesterol homeostasis (Castrillo and Tontonoz, 2004; Repa and Mangelsdorf, 2002). In response to lipoprotein uptake via scavenger receptors, macrophages activate an LXR-dependent pathway for cholesterol efflux. Unexpectedly, we found that phagocytosis of apoptotic cells also activates LXR, likely through the accumulation of membrane-derived cholesterol. LXR in turn activates transcription of Mer, thereby providing positive feedback to promote further clearance, as well as genes such as *Abca1* and *Abcg1* to promote efflux of the excess cholesterol (Tontonoz and Mangelsdorf, 2003). At the same time, LXR activation in response to apoptotic cells also suppresses the production of inflammatory mediators. Since cholesterol is not a component of pathogens such as bacteria, activation of LXR by apoptotic cell-derived cholesterol provides a mechanism to suppress inflammatory responses in some phagocytic pathways but permit them in others.

Collectively, our data provide a new physiological context in which to view the dual activation and transrepression functions of LXR. Activation of genes such as *Abca1* fits well with the established function of this receptor in cholesterol homeostasis. The biological significance of LXR's transrepressive function, however, has been less clear. Is the ability to repress inflammatory gene expression related to cholesterol metabolism, or is this an activity that evolved for a completely separate purpose? We have shown that the process of apoptotic cell clearance integrates both direct gene activation and transrepression and that, at least in this context, inhibition of inflammatory gene expression is intimately linked to metabolism of apoptotic cell lipids. These results illustrate that the activation and transrepression functions of LXR are both important for normal immune homeostasis.

Considerable data support the idea that defective clearance of apoptotic cells leads to autoimmunity (Henson and Hume, 2006; Savill et al., 2002; Vaux and Flavell, 2000). For example, SLE patients exhibit an impaired ability to clear apoptotic cells, and corpses and DNA remnants are found in their serum (Herrmann et al., 1998; Kalden, 1997; Licht et al., 2004). In mice lacking Mfge8, Mer or C1q, lupus-like manifestations have been linked to inefficient removal of apoptotic cells (Botto et al., 1998; Cohen et al., 2002; Hanayama et al., 2004). We have shown that loss of LXR-dependent regulation of Mer and inappropriate activation of inflammatory signaling during phagocytosis leads to the development of autoimmune disease. Interestingly, *Mer*-/- and *Lxr*αβ-/- mice share a number of striking similarities, including exacerbated inflammatory responses and increased susceptibility to both autoimmunity and atherosclerosis (Ait-Oufella et al., 2008; Camenisch et al., 1999; Cohen et al., 2002; Joseph et al., 2003; Thorp et al., 2008). At the same time, the fact that autoimmune disease is more severe in *Lxr*αβ-/- compared to *Mer* -/- mice suggests that more than one LXR-dependent pathway may be involved. We have recently shown that loss of LXRβ leads to increased lymphocyte proliferation (Bensinger et al., 2008). It is likely that the phenotype of *Lxr*αβ-/- mice reflects both the action of LXRα and LXRβ in antigen presenting cells as well as the autonomous effect of LXRβ in lymphocytes. It is also possible that loss of regulation of ABCA1, ApoE (Grainger et al., 2004; Hamon et al., 2000) and other targets contributes to the autoimmune phenotype of LXR null mice. The question of whether defects in the LXR signaling pathway may contribute to the development of human autoimmune disease remains to be investigated.

Finally, we have shown that pharmacological LXR activation has beneficial effects on the progression of autoimmune disease in mouse models of lupus-like disease. A previous study reported that a different LXR agonist slowed the development of disease in an experimental autoimmune encephalomyelitis model, although the underlying mechanism was not addressed (Hindinger et al., 2006). Our studies indicate that LXR activation may compensate for the macrophage phagocytic defect characteristic of lupus-like autoimmunity. In addition, it is likely that the ability of LXRs to directly suppress inflammation and inhibit lymphocyte proliferation also contribute to the therapeutic effects of LXR agonists in these disease models. Further studies will be required to explore the possibility that LXR agonists may have utility in the therapy of human autoimmune disease.

Experimental Procedures

Animals

*Lxr*αβ+/+ and *Lxr*αβ-/- mice on mixed Sv129/C57Bl/6 and C57Bl/6 (backcrossed more than ten generations) backgrounds were provided by David Mangelsdorf (UTSW)(Peet et al., 1998). C57Bl/6 ApoE-/- mice were purchased from Jackson Laboratories. C57Bl/6 *Abcg1*-/- and Sv129/C57Bl/6 *Abca1*-/- mice and their WT controls have been described previously (Kennedy et al., 2005; Timmins et al., 2005). Mice congenic for the spontaneous mutation *Fas*^{lpr} (B6$^{lpr/lpr}$) were purchased from the Jackson Laboratory. For LXR ligand treatment in vivo, WT or autoimmune prone mice were fed a standard chow diet with or without 20 mg/kg/day GW3965. Age-matched female B6$^{lpr/lpr}$ mice were maintained on diet for 4 months. For imaging studies, mice were sedated, injected with PET probe L-FMAC and PET/CT imaging was performed as previously reported (Radu et al., 2008). Images were analyzed using AMIDE software. All mice were maintained under pathogen-free conditions in the animal facilities of the University of California, Los Angeles (UCLA) and University of Las Palmas (ULPGC). Urine samples were collected from individual metabolic cages (kindly donated by L. Fernandez-Perez) and analyzed at the Servicio de Bioquimica Hospital Insular. All animal studies were conducted in accordance with the UCLA and ULPGC Animal Research Committees.

Reagents

The following antibodies and conjugates were used in this study: Mucosal addressin cell adhesion molecule (MAdCAM-1, eBioscience) CD68 (clone FA-11; Serotec), anti-CD4 (clone H129.19; BD Pharmingen), anti-CD8α (clone 53-6.7; BD Pharmingen), anti-CD45R (B220, clone RA3-6B2; Ebioscience), anti-mouse-Mer (R&D Systems), Alexa Fluor 647-anti-F4/80 (clone BM8; eBiosciences), rat anti-mouse F4/80 (kindly provided by S. Gordon and M. Stacey), anti-CD11b-FITC (Clone m1/70; Pharmingen), anti-mouse-IgG-FITC (Sigma), Alexa Fluor 488-anti-rat-IgG and IgM (Molecular probes), Alexa Fluor 594-anti-rat-IgG and IgM (Molecular probes), Alexa Fluor 350-anti rat-IgG, Anti-Rat byotinilated immunoglobulin, (Dako Cytomation). Anti-mouse CD25 (PC61), CD3 (2C11), CD4 (RM4-5), CD8 (53-6.7), CD28 (37.51), CD69 (HI.2F3), Foxp3 (FJK-16s), CD19 (1D3), CD11c (N418), CD11b (M1/70) and F4/80 (BM8) purchased from BD biosciences. FITC-peanut agglutinin (PNA) was purchased from Vector laboratories. CellTracker™ Green CMFDA (5-chloromethylfluorescein diacetate) and CellTracker™ Red CMTPX from Molecular probes were used to stain viable cultured cells in vitro. To quantify free apoptotic cells in culture or from tissues, Annexin V-FITC Apoptosis Detection Kit from BD Pharmingen was used. Apoptotic cells in tissues were also identified by TUNEL reaction following the instructions of the manufacturer with an *In situ* Cell Death Detection Kit, from Roche. Fluorescent Latex beads, carboxilate-modified polystyrene yellow-green (Sigma) and GFP-E.coli (a gift from G. Cheng, UCLA) were used for phagocytosis assays.

Cell Culture and Transfections

Bone marrow-derived macrophages (BMDM) and thioglycolate (TG)-elicited peritoneal macrophages were obtained as described (Castrillo et al., 2003b). Macrophages were cultured in RPMI or DMEM containing 10% fetal bovine serum (FBS, Omega Scientific). For ligand treatments, cells were cultured in medium supplemented with 0.5% BSA and receptor ligands in DMSO vehicle. RAW-LXRα and RAW-FLAG-LXRα stable cell line were generated by retroviral transduction using a pBabe-puro based expression vector as previously described (Chen et al., 2006; Venkateswaran et al., 2000). RAW-Mer stable cell lines were generated by cotransfection of a pCDNA-Mer expression vector (kindly provided by DK Graham) along with a G418 resistance plasmid (Graham et al., 1995). Multiple clones were selected and analyzed for Mer mRNA expression and two independent clones were chosen for analysis. Knockdown studies were performed in RAW-LXRα cells using Amaxa Nucleofection kit specific for mouse macrophages and different specific murine MER siRNAs (Dharmacon) or non-specific siRNA following the following the instructions of the manufacturer. Transfection efficiency was determined by GFP expressing cells. An average of 50-60% transfection efficiency was achieved with this method. Studies with MER blocking antibody were performed in WT and *Lxr*αβ-/- macrophages. 50 μg/ml of anti-Mer antibody (R&D systems) was added to RPMI medium for 3h before phagocytosis assays (see below).

In vitro phagocytosis assays

In vitro phagocytosis assays with mouse macrophages were carried out essentially as described (Hanayama et al., 2002; Scott et al., 2001; Yamauchi et al., 2004). Primary peritoneal macrophages were recovered from mice injected with 3% thyoglicolate for three days. Cells were pelleted and resuspended in RPMI (Cambrex) medium suplemented with 10%FCS (Lonza) and 5×10^5 cells were plated on sterile glass cover-slips. To generate apoptotic thymocytes (AT), thymi from 3- to 4- week-old C57BL/6 mice were harvested and mechanically disociated, filtered, pelleted and resuspended in RPMI medium suplemented with 10%FCS. Apoptosis was induced by treatment with 1 μM of dexamethasone (Sigma) for 6 h. This method results in 60-80% thymocyte apoptosis, as measured with FITC-AnnexinV staining (BD). AT were washed twice with PBS and fluorescein labelled with CellTracker

green (Invitrogen) following manufacturer's instructions. Fluorescent AT were added to peritoneal macrophages in a 5:1 ratio (AT:macrophages) and cultured at 37°C for 30, 60 or 90 min in RPMI supplemented with 10%FBS. Following incubation with AT, macrophages were gently washed several times with cold PBS and Cell Dissociation Buffer, Enzyme Free PBS-based (Invitrogen) to remove free apoptotic thymocytes as described (Krysko et al., 2006; Yamauchi et al., 2004). Cells were then fixed with 2% paraformaldehyde, and phagocytosis was scored using confocal fluorescent microscopy. Phagocytosis was expressed as phagocytic index (PI): number of cells ingested per total number of macrophages × 100 (Fadok et al., 1998; Hanayama et al., 2004). Alternatively, thymocytes were stained with CellTracker red and macrophages were visualized with anti-F4/80 antibody. In some studies, macrophages were treated with 1 μM synthetic LXR agonist (GW3965) in RPMI supplemented with 0.5% FCS prior to addition of apoptotic cells and phagocytosis assays were performed as describe above in RPMI containing 10%FBS. Latex beads and Bacterial phagocytosis were performed with 1 μm Carboxilate-coated fluorescent beads (Sigma) and GFP-*E.Coli* respectively and cultured with macrophages for 30 min. In some experiments sterol content from apoptotic cells was decreased by treating apoptotic thymocytes with methyl-ß-cyclodextrin (MßCD, Sigma). AT were cultured with 5mM of MßCD in RPMI for 1h and then proceed with the phagocytosis assay.

In vivo phagocytosis assays

For *in vivo* peritoneal macrophage phagocytosis assays, 1×10^7 CFSE-labeled apoptotic thymocytes were injected i.p. into 6-8 week-old wild type and *Lxrα*β-/-, *ApoE*-/-, *Abcg1*-/-, *Abca1* WT or *Abca1*-/- mice. Mice were sacrificed after 1 h, and the peritoneum was flushed with 5 ml of PBS. A single cell suspension of peritoneal flush was stained with anti-F4/80 and CD19 to identify macrophage and B cell populations respectively. Cells were analyzed by flow cytometry (described below). Statistical analysis was performed using Student's T-test.

For *in vivo* thymic phagocytosis assays, 4-week-old mice were injected i.p. with 0.2 mg of dexamethasone per 25 g body weight in PBS (Sigma). After 24 h, mice were sacrificed and thymi were extracted and mechanically dissociated. Free apoptotic cells were determined with FITC-AnnexinV staining using a Coulter Epics XL-MCL (Beckman Coulter). Additionally, cells were fixed, permeabilized and total apoptotic cells were measured using the TUNEL reaction (*In situ* cell death detection Kit from Roche). For transmission electron microscopy analysis, mice treated for 24 h with dexamethasone were sacrificed and perfused with fixation solution (2% glutaraldehyde). Thymi were harvested, fixed with 2% OsO_4, dehydrated and embedded in epoxy resin**.** Ultra-thin sections were stained with uranyl acetate and lead citrate and observed under electron microscope at the ULPGC electron microscopy core facility.

Histology

Tissues were collected and fixed in 4% buffered formalin, dehydrated in successive alcohol solutions, embedded in paraffin wax and sectioned for H&E staining. Alternatively, tissues were directly collected from the animal, embedded in OCT compound (Tissue-Tek) and snap-frozen in liquid Nitrogen and Isopentane. 4 μm frozen sections were air-dried, fixed with 4% paraformaldehyde, blocked with 6% BSA and 2% preimmune serum in PBS and stained with fluorescence conjugated antibodies diluted in blocking solution; nuclei were stained with DAPI (Vectashield mountain medium fluorescence with DAPI, Vector). For non-fluorophore-conjugated antibodies, biotinilated secondary antibodies were visualized using the streptavidin-biotin-peroxidase method (Vectastain ABC Kit, Vector laboratories) and stained with the cromogen 3-3′-diaminobenzidine tetrahydrochloride (DAB Substrate Kit for peroxidase, Vector laboratories). Nuclei were counterstained with hematoxilin. TUNEL reaction (*In situ* cell death detection kit from Roche), was used to identify apoptotic cells in frozen sections from spleen, thymus, lung, and testis: 4 μm sections were fixed with 2%

paraformaldehyde, permeabilized with 0.1% Triton X100 in 0.1% sodium citrate and stained with the TUNEL reaction. Then, macrophages were identified in the same sections using rat anti-mouse-CD68 (Serotec) and visualized with secondary antibody anti-rat-Alexa Fluor 594 (Molecular Probes). Sections and pictures were observed under a Zeiss LSM 5 PASCAL Laser Scaning Microscope (Carl Zeiss, Germany).

ELISA and biochemical parameters

The presence of antinuclear antibodies ANA (using a Mesacup ANA test from MBL), and autoantibodies directed against dsDNA, and histones were examined in serial dilutions of mouse serum by ELISA as described in previously (Salvador et al., 2002). Briefly, 96-well flat-bottom plates (Nunc-immuno plate F96 MAXISORP) were precoated with 2.5 μg of poly-L-lysine (Sigma) for 1 hr at 37°C. Plates were incubated with 0.5 μg/well of dsDNA, histone type II-S from calf thymus (Sigma) overnight at 4° C. After blocking the nonspecific sites with 5% FCS for 1 h at 37° C, mice serum samples were added for 3 h at room temperature. Then followed 1 h of incubation with HRP-labeled goat anti-mouse IgG Fc-specific (Jackson Immunoresearch) diluted 1:500. A substrate solution containing equal volumes of Sigma Fast OPD peroxidase substrate was added. After incubation of 5min at room temperature, reaction was stopped with 50 μl of 3M H_2SO_4 solution and the plates were read at 492 nm in ELISA reader (Bio-Rad).

DNA, RNA, and Protein Analysis

Total RNA was harvested using TRIzol reagent (Invitrogen). Total RNA was reverse-transcribed with random hexamers by using iScript reverse-transcription reagents kit (Bio-Rad) according to manufacturer protocol. Real-time quantitative PCR (SYBRgreen) assays were performed using an Applied Biosystems 7900 sequencer detector as described previously (Joseph et al., 2003; Laffitte et al., 2001). Expression was normalized to 36B4 expression. Primer and probe sequences are available upon request. Statistical analysis of mRNA expression data were performed by using the Student's t test. Probe and primer sequences are available on request. Electrophoretic Mobility Shift Assay was performed as described previously (Laffitte et al., 2001). Briefly, murine LXRα and RXRα proteins were synthesized using the TnT T7 quick-coupled transcription/translation system (Promega). Reaction mixture containing proteins and buffer was briefly preincubated with RXRα polyclonal antibody (Santa Cruz Biotechnology) before addition of radiolabeled oligonucleotides as indicated. The binding reactions were resolved on a pre-electrophoresed 1X TBE, 5% polyacrylamide gel. Oligonucleotides used were as follows (only one strand shown): Mer LXRE primer: 5′-ttcatgtgtatgctggggtaccca-3′, Mer Mutant LXRE: 5′-ttcattttaatgcagtttaaccca-3′, and SREBP1c LXRE: 5′-cgctggggttactggcggtcactgta-3′. For Northern blots, 10 μg of total RNA isolated from cells, was separated by gel electrophoresis, transferred to nylon membranes, and hybridized with [α-^{32}P]dCTP-labeled DNA probes as described (Castrillo et al., 2003b).

Chromatin immunoprecipitation (ChIP) assays were performed essentially as described (Hecht and Grunstein, 1999). Briefly, RAW-LXRα or RAW-FLAG- LXRα macrophages were cultured with GW3965 for 1 h and fixed with 1% formaldehyde. After cross-linking, cells were sonicated in order to obtain DNA fragments of 300-1000 bp. Immunoprecipitation was performed by using the following antibodies: anti-NCoR (Affinity Bioreagents, Golden, Colo.) and rabbit anti-RNA PolII, anti RXRα, anti-FLAG, anti-Rabbit IgG (Santa Cruz Biotechnology). Protein-DNA complexes were reverse cross-linked at 65°C overnight and DNA was purified using a PCR purification kit (G&E Healthcare). Fractions of DNA were used for real-time quantitative PCR.

For western blot analysis, whole cell lysates were boiled and separated on a SDS-PAGE gel. Proteins were transferred onto polyvinylidene difluoride membrane (Amersham), blocked in

TBS with 0,1% Tween20 and 5% milk, incubated with the following antibodies. Rabbit anti Mer and ABCG1 from Novus Biologicals, rabbit ABCA1 antisera was kindly provided by Michael L. Fitzgerald (Fitzgerald et al., 2001) (MGH, Boston MA) and rabbit anti-ApoE from AbCAM and secondary goat anti-rabbit HRP from Amersham. Blots were washed in TBS-T and visualized with ECL-Plus (Amersham Biosciences) and Bio-Rad Chemi-Doc imaging system.

DNA Microarray Analysis

Total RNA was isolated from RAW264.7 macrophages ectopically expressing LXRα (Venkateswaran et al., 2000) cultured with vehicle or GW3965 (1 μM) and LG268 (100 nM). Transcriptional profiling was performed at the UCLA microarray core facility using murine Affymetrix 430 2.0 microarrays. Data was analyzed using GeneSpring and GeneChip Analysis Suite software (Affymetrix) as described previously (Zelcer et al., 2007). Only statistically significant expression differences are presented.

Flow Cytometry

Single cell suspensions from lymph nodes and spleens were obtained from mice and washed twice in staining buffer, resuspended and incubated with labelled antibodies diluted in staining buffer for 30 min at 4°C. After incubation cells were washed in staining buffer and analyzed immediately. Intracellular FoxP3 staining was performed per Manufactures instruction (ebiosciences). Cells were analyzed on FACSCalibur or LSRII (Becton-Dickinson) using FlowJo software (Treestar, Inc.). For *in vivo* thymic phagocytosis assay and for *in vitro* apoptosis analysis of thymocytes, TUNEL reaction and FITC-AnnexinV staining were analyzed on Coulter Epics XL-MCL (Beckman Coulter).

Statistical analysis

Data were expressed as mean ± SD. Statistical analysis was performed using Student's *t* test for two samples. For multiple comparisons, data were evaluated by one-way analysis of variance (ANOVA). Values of $P < 0.05$ were considered to be significant.

Supplementary Material

Refer to Web version on PubMed Central for supplementary material.

Acknowledgments

We thank D. Mangelsdorf for the *Lxr* null mice; J. Collins and T. Willson for GW3965 and D.K. Graham, P.M. Henson, S. Gordon, G. Cheng, ML Fitzgerald**,** J.M. Salvador, L. Fernandez-Perez, A. Corbí, A. Tugores, F. Díaz-Gonzalez and L. Bosca for key reagents and comments. We thank C. Radu and R. Laing for their assistance with the PET imaging studies. We also thank R. Hernandez for technical assistance. This work was supported by grants from the Spanish CSIC, MICINN of I+D SAF2005-03270 and 2008-00057, Ramon y Cajal Program, BM05-228 from "La Caixa" and Ramon Areces Foundations to A.C. and from the NIH to P.T. (HL066088), P.E. (HL030568) and J.P. (HL049373). N.A.G., S.B., J.D. are supported by training grants from Ramon Areces, MEC and Cabildo Gran Canaria respectively. C.R. is supported by a postdoctoral fellowship from Consejeria Industria. Flow cytometry was performed at the UCLA Core Facility supported by CA16042 and AI28697. Imaging was performed at the In Vivo Cellular and Molecular Imaging Center supported by EB001943 and CA92865. P.T. is an Investigator and C.H. is a Research Associate of the Howard Hughes Medical Institute.

References

Ait-Oufella H, Pouresmail V, Simon T, Blanc-Brude O, Kinugawa K, Merval R, Offenstadt G, Lesèche G, Cohen P, Tedgui A, et al. Defective Mer Receptor Tyrosine Kinase Signaling in Bone Marrow Cells Promotes Apoptotic Cell Accumulation and Accelerates Atherosclerosis. Arterioscler Thromb Vasc Biol 2008;8:1429–31. [PubMed: 18467644]

Bensinger SJ, Bradley MN, Joseph SB, Zelcer N, Janssen EM, Hausner MA, Shih R, Parks JS, Edwards PA, Jamieson BD, et al. LXR signaling couples sterol metabolism to proliferation in the acquired immune response. Cell 2008;134:97–111. [PubMed: 18614014]

Botto M, Dell'Agnola C, Bygrave A, Thompson E, Cook HT, Petry F, Loos M, Pandolfi PP, Walport MJ. Homozygous C1q deficiency causes glomerulonephritis associated with multiple apoptotic bodies. Nat Genet 1998;19:56–59. [PubMed: 9590289]

Camenisch TD, Koller B, Earp HS, Matsushima GK. A novel receptor tyrosine kinase, Mer, inhibits TNF-alpha production and lipopolysaccharide-induced endotoxic shock. J Immunol 1999;162:3498–3503. [PubMed: 10092806]

Castrillo A, Joseph SB, Marathe C, Mangelsdorf DJ, Tontonoz P. Liver X receptor-dependent repression of matrix metalloproteinase-9 expression in macrophages. J Biol Chem 2003a;278:10443–10449. [PubMed: 12531895]

Castrillo A, Joseph SB, Vaidya SA, Haberland M, Fogelman AM, Cheng G, Tontonoz P. Crosstalk between LXR and toll-like receptor signaling mediates bacterial and viral antagonism of cholesterol metabolism. Mol Cell 2003b;12:805–816. [PubMed: 14580333]

Castrillo A, Tontonoz P. Nuclear receptors in macrophage biology: at the crossroads of lipid metabolism and inflammation. Annu Rev Cell Dev Biol 2004;20:455–480. [PubMed: 15473848]

Cohen PL, Caricchio R, Abraham V, Camenisch T, Jennette JC, Roubey RA, Earp HS, Matsushima G, Reap E. Delayed apoptotic cell clearance and lupus-like autoimmunity in mice lacking the c-mer membrane tyrosine kinase. J Exp Med 2002;196:135–140. [PubMed: 12093878]

Collins JL, Fivush AM, Watson MA, Galardi CM, Lewis M, Moore L, Parks D, Wilson J, Tippin TK, Binz JG, et al. Identification of a nonsteroidal liver X receptor agonist through parallel array synthesis of tertiary amines. J Med Chem 2002;45:1963–1966. [PubMed: 11985463]

Chen M, Bradley MN, Beaven SW, Tontonoz P. Phosphorylation of the liver X receptors. FEBS Lett 2006;580:4835–4841. [PubMed: 16904112]

Fadok V, Bratton D, Konowal A, Freed P, Westcott J, Henson P. Macrophages that have ingested apoptotic cells in vitro inhibit proinflammatory cytokine production through autocrine/paracrine mechanisms involving TGF-beta, PGE2, and PAF. J Clin Invest 1998;101:890–898. [PubMed: 9466984]

Fadok VA, Warner ML, Bratton DL, Henson PM. CD36 is required for phagocytosis of apoptotic cells by human macrophages that use either a phosphatidylserine receptor or the vitronectin receptor (alpha v beta 3). J Immunol 1998;161:6250–6257. [PubMed: 9834113]

Fitzgerald ML, Mendez AJ, Moore KJ, Andersson LP, Panjeton HA, Freeman MW. ATP-binding cassette transporter A1 contains an NH2-terminal signal anchor sequence that translocates the protein's first hydrophilic domain to the exoplasmic space. J Biol Chem 2001;276:15137–15145. [PubMed: 11328826]

Ghisletti S, Huang W, Ogawa S, Pascual G, M L, Willson TM, Rosenfeld MG, Glass CK. Parallel SUMOylation-dependent pathways mediate gene- and signal-specific transrepression by LXRs and PPARgamma. Mol Cell 2007;25:57–70. [PubMed: 17218271]

Graham DK, Bowman GW, Dawson TL, Stanford WL, Earp HS, Snodgrass HR. Cloning and developmental expression analysis of the murine c-mer tyrosine kinase. Oncogene 1995;10:2349–2359. [PubMed: 7784083]

Grainger DJ, Reckless J, McKilligin E. Apolipoprotein E modulates clearance of apoptotic bodies in vitro and in vivo, resulting in a systemic proinflammatory state in apolipoprotein E-deficient mice. J Immunol 2004;173:6366–6375. [PubMed: 15528376]

Green D. apoptotic signaling pathways in the immune system. Immunol Rev 2003;193:5–9. [PubMed: 12752665]

Grimsley C, Ravichandran K. Cues for apoptotic cell engulfment: eat-me, don't eat-me and come-get-me signals. Trends Cell Biol 2003;13:648–656. [PubMed: 14624843]

Hamon Y, Broccardo C, Chambenoit O, Luciani M, Toti F, Chaslin S, Freyssinet J, Devaux P, McNeish J, Marguet D, et al. ABC1 promotes engulfment of apoptotic cells and transbilayer redistribution of phosphatidylserine. Nat Cell Biol 2000;2:399–406. [PubMed: 10878804]

Hanayama R, Tanaka M, Miwa K, Shinohara A, Iwamatsu A, Nagata S. Identification of a factor that links apoptotic cells to phagocytes. Nature 2002;417:182–187. [PubMed: 12000961]

Hanayama R, Tanaka M, Miyasaka K, Aozasa K, Koike M, Uchiyama Y, Nagata S. Autoimmune disease and impaired uptake of apoptotic cells in MFG-E8-deficient mice. Science 2004;304:1147–1150. [PubMed: 15155946]

Hecht A, Grunstein M. Mapping DNA interaction sites of chromosomal proteins using immunoprecipitation and polymerase chain reaction. Methods Enzymol 1999;304:399–414. [PubMed: 10372373]

Henson P, Bratton D, Fadok V. Apoptotic cell removal. Curr Biol 2001;11:795–805.

Henson P, Hume D. Apoptotic cell removal in development and tissue homeostasis. Trends Immunol 2006;27:244–250. [PubMed: 16584921]

Herrmann M, Voll RE, Zoller OM, Hagenhofer M, Ponner BB, Kalden JR. Impaired phagocytosis of apoptotic cell material by monocyte-derived macrophages from patients with systemic lupus erythematosus. Arthritis Rheum 1998;41:1241–1250. [PubMed: 9663482]

Hindinger C, Hinton DR, Kirwin SJ, Atkinson RD, Burnett ME, Bergmann CC, Stohlman SA. Liver X receptor activation decreases the severity of experimental autoimmune encephalomyelitis. J Neurosci Res 2006;84:1225–1234. [PubMed: 16955483]

Ishimoto Y, Ohashi K, Mizuno K, Nakano T. Promotion of the uptake of PS liposomes and apoptotic cells by a product of growth arrest-specific gene, gas6. J Biochem 2000;127:411–417. [PubMed: 10731712]

Joseph SB, Bradley MN, Castrillo A, Bruhn KW, Mak PA, Pei L, Hogenesch J, O'Connell R M, Cheng G, Saez E, et al. LXR-dependent gene expression is important for macrophage survival and the innate immune response. Cell 2004;119:299–309. [PubMed: 15479645]

Joseph SB, Castrillo A, Laffitte BA, Mangelsdorf DJ, Tontonoz P. Reciprocal regulation of inflammation and lipid metabolism by liver X receptors. Nat Med 2003;9:213–219. [PubMed: 12524534]

Kalden J. Defective phagocytosis of apoptotic cells: possible explanation for the induction of autoantibodies in SLE. Lupus 1997;6:326–327. [PubMed: 9296780]

Kennedy MA, Barrera GC, Nakamura K, Baldan A, Tarr P, Fishbein MC, Frank J, Francone OL, Edwards PA. ABCG1 has a critical role in mediating cholesterol efflux to HDL and preventing cellular lipid accumulation. Cell Metab 2005;1:121–131. [PubMed: 16054053]

Krysko DV, Denecker G, Festjens N, Gabriels S, Parthoens E, D'Herde K, Vandenabeele P. Macrophages use different internalization mechanisms to clear apoptotic and necrotic cells. Cell Death Differ 2006;13:2011–2022. [PubMed: 16628234]

Laffitte BA, Joseph SB, Walczak R, Pei L, Wilpitz DC, Collins JL, Tontonoz P. Autoregulation of the human liver X receptor alpha promoter. Mol Cell Biol 2001;21:7558–7568. [PubMed: 11604492]

Lauber K, Blumenthal S, Waibel M, Wesselborg S. Clearance of apoptotic cells: getting rid of the corpses. Mol Cell 2004;14:277–287. [PubMed: 15125832]

Lauber K, Bohn E, Krober SM, Xiao YJ, Blumenthal SG, Lindemann RK, Marini P, Wiedig C, Zobywalski A, Baksh S, et al. Apoptotic cells induce migration of phagocytes via caspase-3-mediated release of a lipid attraction signal. Cell 2003;113:717–730. [PubMed: 12809603]

Lemke G, Rothlin C. Immunobiology of the TAM receptors. Nat Rev Immunol 2008;8:327–336. [PubMed: 18421305]

Li M, Flavell R. Contextual regulation of inflammation: a duet by transforming growth factor-beta and interleukin-10. Immunity 2008;28:468–476. [PubMed: 18400189]

Licht R, Dieker J, Jacobs C, Tax W, Berden J. Decreased phagocytosis of apoptotic cells in diseased SLE mice. J Autoimmun 2004;22:139–145. [PubMed: 14987742]

Miyanishi M, Tada K, Koike M, Uchiyama Y, Kitamura T, Nagata S. Identification of Tim4 as a phosphatidylserine receptor. Nature 2007;450:435–439. [PubMed: 17960135]

O'Shea J, Ma A, Lipsky P. Cytokines and autoimmunity. Nat Rev Immunol 2002;2:37–45. [PubMed: 11905836]

Peet DJ, Turley SD, Ma W, Janowski BA, Lobaccaro JM, Hammer RE, Mangelsdorf DJ. Cholesterol and bile acid metabolism are impaired in mice lacking the nuclear oxysterol receptor LXR alpha. Cell 1998;93:693–704. [PubMed: 9630215]

Potter PK, Cortes-Hernandez J, Quartier P, Botto M, Walport MJ. Lupus-prone mice have an abnormal response to thioglycolate and an impaired clearance of apoptotic cells. J Immunol 2003;170:3223–3232. [PubMed: 12626581]

Qian Y, Conway KL, Lu X, Seitz HM, Matsushima GK, Clarke SH. Autoreactive MZ and B-1 B-cell activation by Faslpr is coincident with an increased frequency of apoptotic lymphocytes and a defect in macrophage clearance. Blood 2006;108:974–982. [PubMed: 16861350]

Rabinowitz SS, Gordon S. Macrosialin, a macrophage-restricted membrane sialoprotein differentially glycosylated in response to inflammatory stimuli. J Exp Med 1991;174:827–836. [PubMed: 1919437]

Radu CG, Shu CJ, Nair-Gill E, Shelly SM, Barrio JR, Satyamurthy N, Phelps ME, Witte ON. Molecular imaging of lymphoid organs and immune activation by positron emission tomography with a new [18F]-labeled 2′-deoxycytidine analog. Nat Med 2008;14:783–788. [PubMed: 18542051]

Ravichandran KS, Lorenz U. Engulfment of apoptotic cells: signals for a good meal. Nat Rev Immunol 2007;7:964–974. [PubMed: 18037898]

Repa JJ, Mangelsdorf DJ. The liver X receptor gene team: potential new players in atherosclerosis. Nat Med 2002;8:1243–1248. [PubMed: 12411951]

Rothlin CV, Ghosh S, Zuniga EI, Oldstone MB, Lemke G. TAM receptors are pleiotropic inhibitors of the innate immune response. Cell 2007;131:1124–1136. [PubMed: 18083102]

Salvador JM, Hollander MC, Nguyen AT, Kopp JB, Barisoni L, Moore JK, J.D. A, Fornace AJJ. Mice lacking the p53-effector gene Gadd45a develop a lupus-like syndrome. Immunity 2002;16:499–508. [PubMed: 11970874]

Savill J, Dransfield I, Gregory C, Haslett C. A blast from the past: clearance of apoptotic cells regulates immune responses. Nat Rev Immunol 2002;2:965–975. [PubMed: 12461569]

Savill J, Fadok V. Corpse clearance defines the meaning of cell death. Nature 2000;407:784–788. [PubMed: 11048729]

Scott RS, McMahon EJ, Pop SM, Reap EA, Caricchio R, Cohen PL, Earp HS, Matsushima GK. Phagocytosis and clearance of apoptotic cells is mediated by MER. Nature 2001;411:207–211. [PubMed: 11346799]

Sen P, Wallet MA, Yi Z, Huang Y, Henderson M, Mathews CE, Earp HS, Matsushima G, Baldwin AS, Tisch RM. Apoptotic cells induce Mer tyrosine kinase-dependent blockade of NF-kappaB activation in dendritic cells. Blood 2007;109:653–660. [PubMed: 17008547]

Smith JP, Lister AM, Tew JG, Szakal AK. Kinetics of the tingible body macrophage response in mouse germinal center development and its depression with age. Anat Rec 1991;229:511–520. [PubMed: 2048755]

Tangirala RK, Bischoff ED, Joseph SB, Wagner BL, Walczak R, Laffitte BA, Daige CL, Thomas D, Heyman RA, Mangelsdorf DJ, et al. Identification of macrophage liver X receptors as inhibitors of atherosclerosis. Proc Natl Acad Sci U S A 2002;99:11896–11901. [PubMed: 12193651]

Taylor PR, Martinez-Pomares L, Stacey M, Lin HH, Brown GD, Gordon S. Macrophage receptors and immune recognition. Annu Rev Immunol 2005;23:901–944. [PubMed: 15771589]

Thorp E, Cui D, Schrijvers DM, Kuriakose G, Tabas I. Mertk Receptor Mutation Reduces Efferocytosis Efficiency and Promotes Apoptotic Cell Accumulation and Plaque Necrosis in Atherosclerotic Lesions of Apoe-/- Mice. Arterioscler Thromb Vasc Biol. May 1;2008 Epub Ahead of Print

Timmins JM, Lee JY, Boudyguina E, Kluckman KD, Brunham LR, Mulya A, Gebre AK, Coutinho JM, Colvin PL, Smith TL, Hayden MR, Maeda N, Parks JS. Targeted inactivation of hepatic Abca1 causes profound hypoalphalipoproteinemia and kidney hypercatabolism of apoA-I. J Clin Invest 2005;115:1333–42. [PubMed: 15841208]

Tontonoz P, Mangelsdorf DJ. Liver x receptor signaling pathways in cardiovascular disease. Mol Endocrinol 2003;17:985–993. [PubMed: 12690094]

Vaux DL, Flavell RA. Apoptosis genes and autoimmunity. Curr Opin Immunol 2000;12:719–724. [PubMed: 11102778]

Venkateswaran A, Laffitte BA, Joseph SB, Mak PA, Wilpitz DC, Edwards PA, Tontonoz P. Control of cellular cholesterol efflux by the nuclear oxysterol receptor LXR alpha. Proc Natl Acad Sci U S A 2000;97:12097–12102. [PubMed: 11035776]

Voll RE, Herrmann M, Roth EA, Stach C, Kalden JR, Girkontaite I. Immunosuppressive effects of apoptotic cells. Nature 1997;390:350–351. [PubMed: 9389474]

Yamauchi A, Kim C, Li S, Marchal CC, Towe J, Atkinson SJ, Dinauer MC. Rac2-deficient murine macrophages have selective defects in superoxide production and phagocytosis of opsonized particles. J Immunol 2004;173:5971–5979. [PubMed: 15528331]

Zelcer N, Khanlou N, Clare R, Jiang Q, Reed-Geaghan EG, Landreth GE, Vinters HV, Tontonoz P. Attenuation of neuroinflammation and Alzheimer's disease pathology by liver x receptors. Proc Natl Acad Sci U S A 2007;104:10601–10606. [PubMed: 17563384]

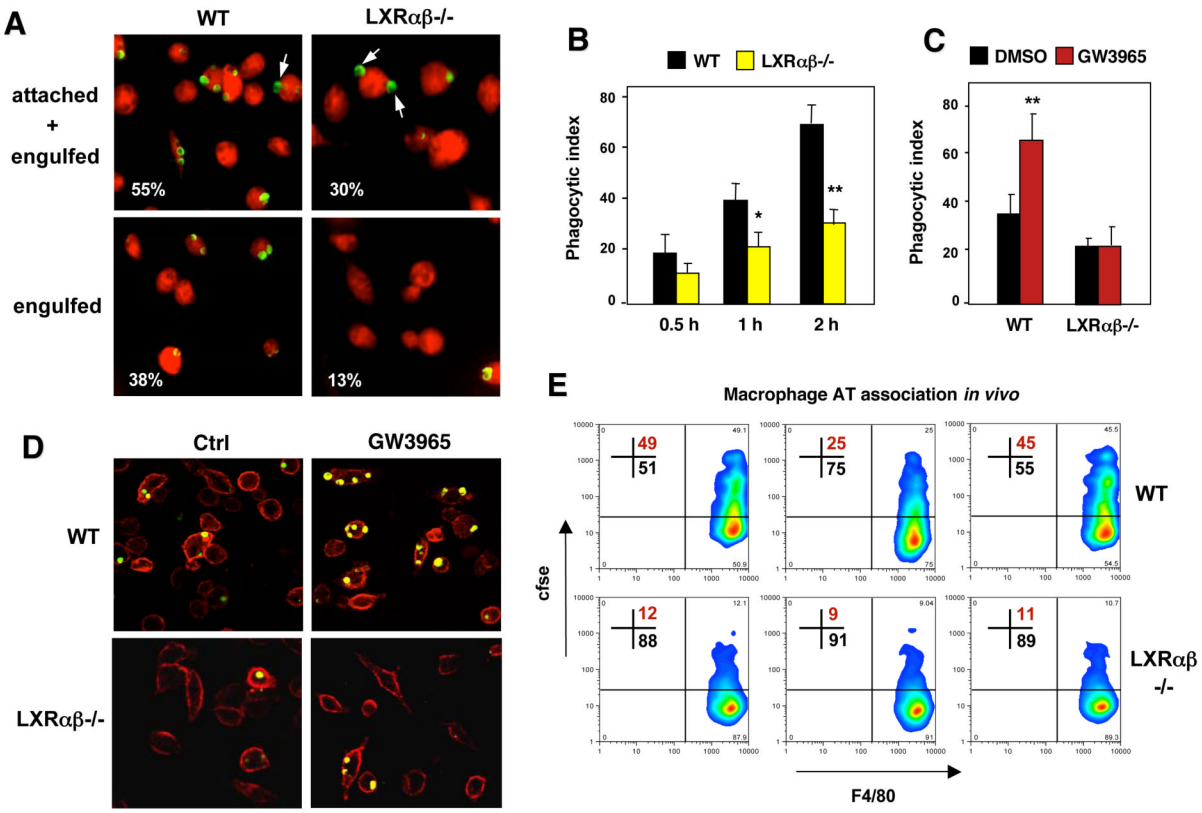

Figure 1. LXR signaling regulates phagocytosis of apoptotic cells

(A). Decreased engulfment of apoptotic thymocytes by *Lxr*αβ-/- macrophages *in vitro* as visualized by phagocytosis of CellTracker™ Green CMFDA-labeled AT. A cell dissociation buffer (Krysko et al., 2006) was added to distinguish engulfed from bound cells as indicated. Arrows indicate attached cells. CellTracker™ Green CMFDA-labeled AT were cultured with macrophages (stained with CellTracker™ Red CMTPX) for 1 h. In this and all subsequent experiments a ratio of 5 AT:1 macrophage was used. Attached and engulfed cells were distinguished by extensive washing with cold PBS and Enzyme Free Cell Dissociation Buffer (Invitrogen) to remove free AT. Macrophage phagocytosis was evaluated by fluorescence microscopy. B) Quantification of phagocytosis by confocal microscopy after incubation of apoptotic thymocytes (AT) for 0.5, 1 or 2 h with WT or LXRαβ-/- macrophages. C,D) LXR agonist promotes phagocytosis of labeled AT as shown by confocal microscopy. Thioglycolate-elicited peritoneal macrophages from WT or LXRαβ-/- mice were pretreated with vehicle or 1 μM GW3965 for 48 h and then incubated with apoptotic cells for 1 h. E) *In vivo* association of csfe-labeled apoptotic cells with WT or *Lxr*αβ-/- macrophages was determined by flow cytometry. Results from 3 separate mice are shown for each genotype. All experiments were repeated a minimum of three times with comparable results. Data were expressed as mean ± SD. Statistical analysis was performed using Student's t test. *P < 0.05, **P < 0.01

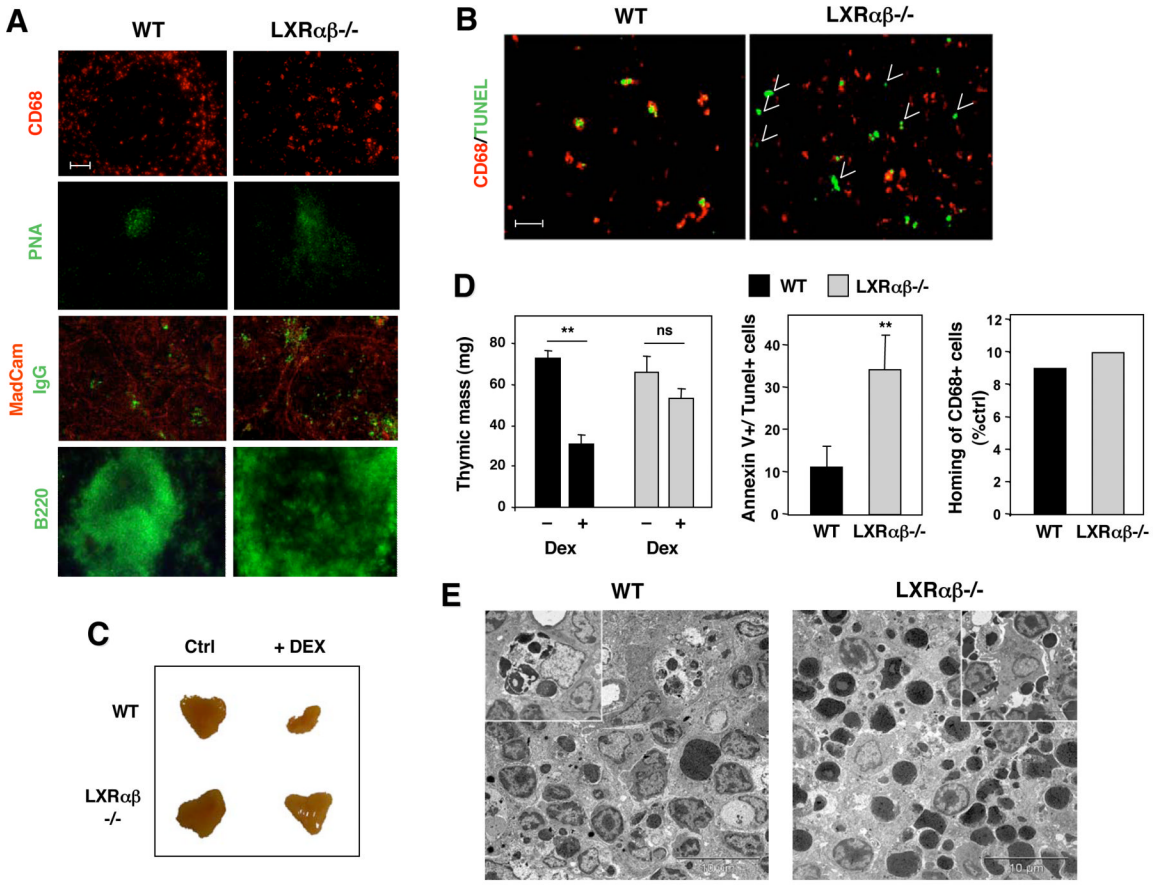

Figure 2. Defective *in vivo* clearance of apoptotic cells in *LXR*αβ-/- lymphoid tissues

A) Spleen sections from 40 week-old WT and *Lxr*αβ-/- mice were stained with fluorescein-labeled peanut agglutinin (PNA), IgG, Mucosal addressin cell adhesion molecule (MAdCAM-1), and B220 as indicated. Bar represents 50 μm. B) Representative spleen sections (4 μm) from 40 week-old WT and LXRαβ-/- mice were analyzed by TUNEL staining (green) and staining for CD68+ macrophages (red). Free apoptotic cells are indicated by arrows (right panel). Bar represents 25 μm. C) 4-week old male WT and LXRαβ-/- mice (4 animals/group) were injected with 0.2 mg dexamethasone (dex) and thymi were isolated 24 h later. D) Thymic mass was measured in each mouse after 24 h of dex. The percentage of Annexin V+/Tunel+ cells and recruitment of macrophages was evaluated in cell suspensions by flow cytometry. E) Thymic sections were analyzed by transmission electron microscopy. **P < 0.001.

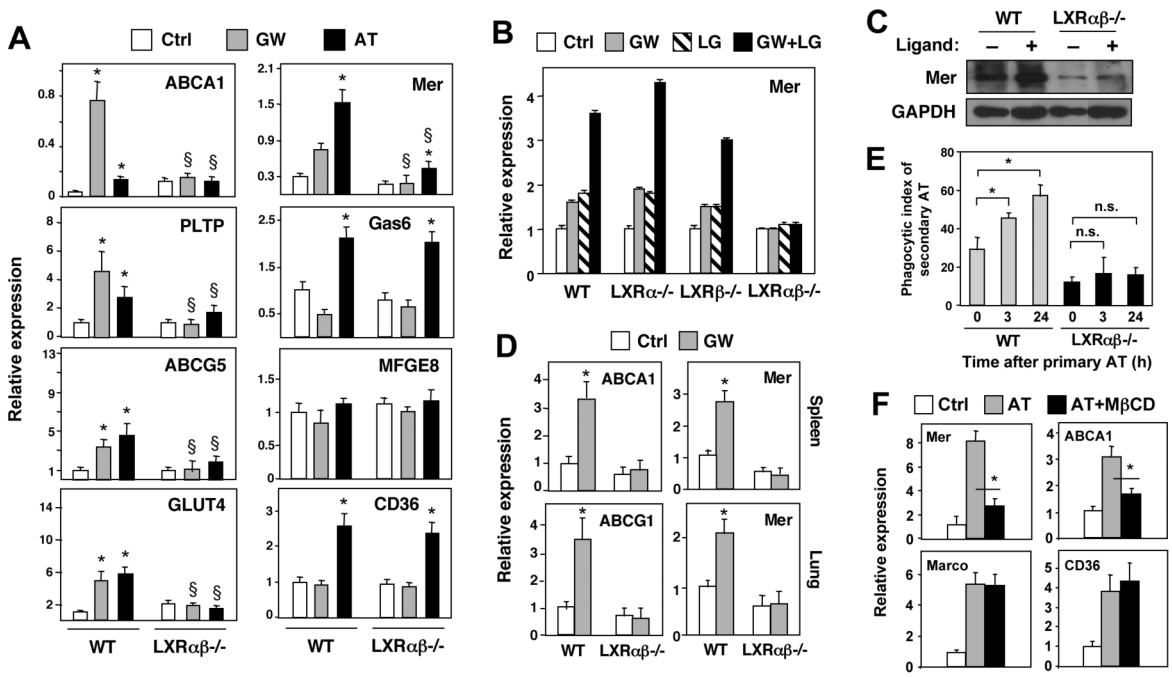

Figure 3. Regulation of Mer expression by LXR/RXR heterodimers. Apoptotic cells promote Mer expression and phagocytosis through LXR-dependent pathways

A) Thioglycolate-elicited peritoneal macrophages from WT or *LXR*αβ-/- mice were treated with vehicle, 1 μM GW3965 (GW), or AT (ratio of 5 AT:1 macrophage) for 24 h. Gene expression was measured by real-time PCR. *P < 0.05 versus vehicle control; §P < 0.05 versus WT control. Experiment was repeated three times with comparable results. B) LXR-dependent regulation of Mer expression in peritoneal macrophages. mRNA expression was assayed in WT, *Lxr*α-/- α-/-, *Lxr*β-/- or *Lxr*αβ-/- macrophages treated for 24 h with 1 μM GW3965 and/or 100 nM LG268 (LG). C) Induction of Mer protein expression by LXR/RXR agonists in primary WT and *Lxr*αβ-/- macrophages. D) Induction of Mer expression *in vivo*. mRNA expression was evaluated in spleen and lung tissues from WT and *LXR*αβ-/- mice treated with GW agonist for 3 days. N=5 per group. *P < 0.05. E) Apoptotic cells promote their own uptake in an LXR-dependent manner. WT or LXRαβ-/- macrophages were challenged with CMFDA-labeled AT for 90 min. 3 or 24 h later, the same macrophages were challenged with a second round of CMTPX-labeled AT for 90 min and only CMTPX-labeled engulfed cells were scored as in Fig 1. *P < 0.05. F). Depletion of cellular sterols from AT inhibits their ability to activate LXR. Sterol content from AT was decreased by treating cells with 5 mM of methyl-beta-cyclodextran (MßCD) prior to addition to macrophages. Macrophages were cultured with untreated or sterol-depleted AT for 90 min. Unengulfed cells were removed and gene expression was measured by real-time PCR after 24 h.

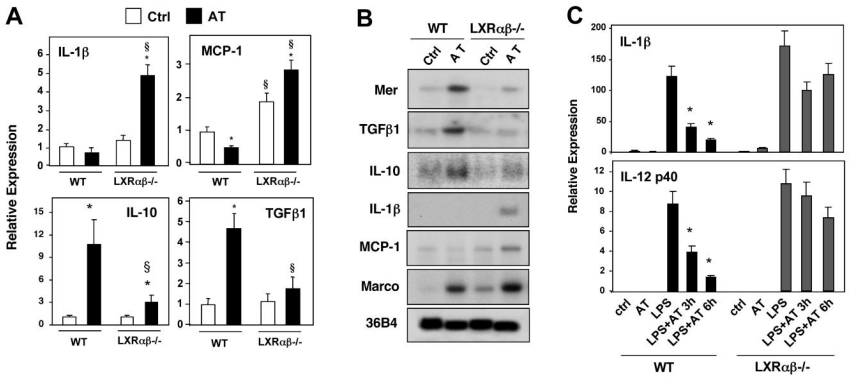

Figure 4. Apoptotic cells promote tolerogenic gene expression and repression of proinflammatory mediators through LXR-dependent pathways

A) Thioglycolate-elicited peritoneal macrophages from WT or *Lxr*αβ-/- mice were treated with vehicle or AT (ratio of 5 AT:1 macrophage) for 24 h. Gene expression was measured by real-time PCR. *P < 0.05 versus vehicle control; §P < 0.05 versus WT control. Experiment was repeated three times with comparable results. B) Macrophages from WT and *Lxr*αβ-/- mice were challenged with AT for 24 h and mRNA expression was evaluated by Northern blotting. C) Exposure to apoptotic cells inhibits macrophage responses to LPS in an LXR-dependent manner. WT or *Lxr*αβ-/- macrophages were preincubated with AT for 1h and then challenged with LPS for 3 and 6h. Gene expression was evaluated by real-time PCR. *P<0.05.

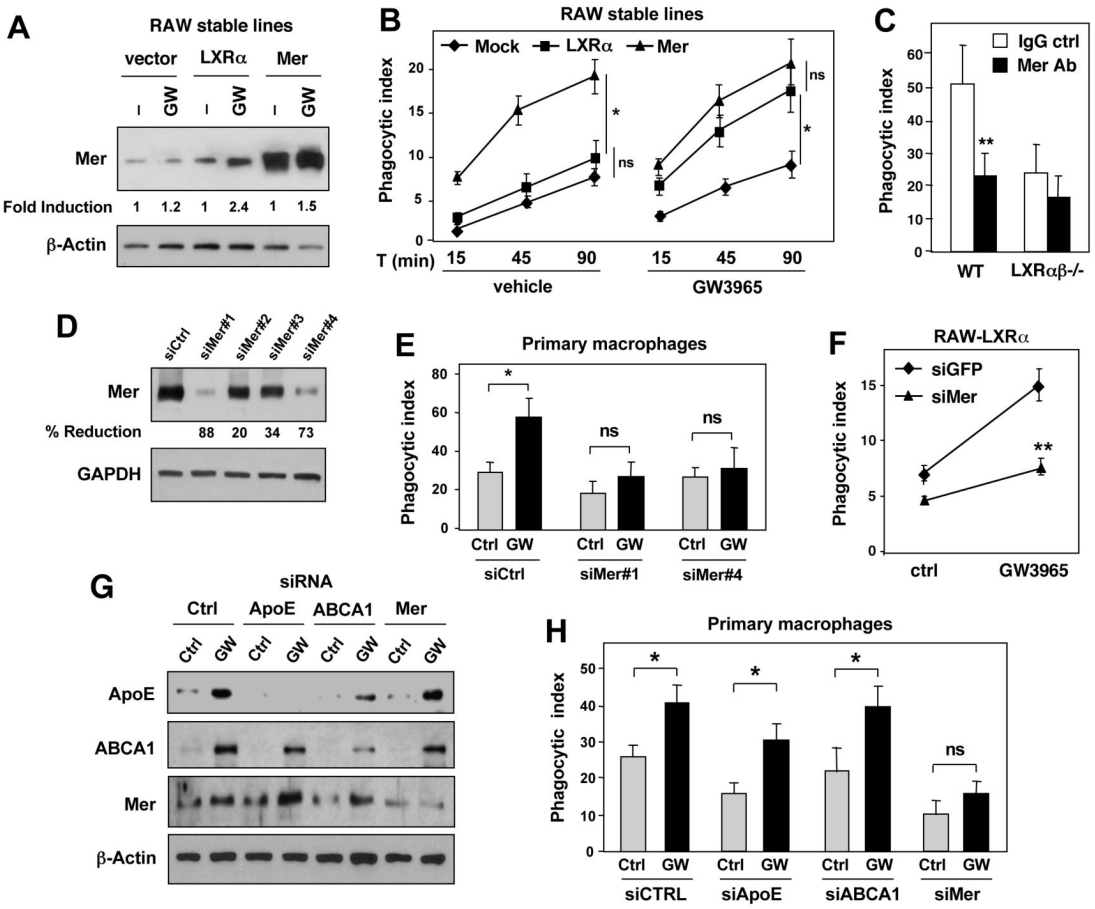

Figure 5. Mer expression is required for LXR-dependent phagocytosis of apoptotic cells

A) Protein expression in RAW cells stably expressing LXRα (RAW-LXRα) or Mer (RAW-Mer). B) Phagocytosis of apoptotic cells was evaluated in RAW-LXRα or RAW-Mer macrophages. Cells were treated for 36 h with GW3965 and then challenged with AT for 15, 45 and 90 min. C) A blocking antibody to Mer inhibits AT uptake in WT but not LXRαβ-/- macrophages. Thioglycolate-elicited peritoneal macrophages from WT or LXRαβ-/- mice were incubated with either IgG control antibody or Mer-specific blocking antibody for 3h. Phagocytosis of apoptotic cells was evaluated by confocal microscopy after 90 min incubation of AT. *P < 0.05. D) Effect of control and Mer-specific siRNAs on protein expression in RAW cells. E) Mer knockdown blocks the effect of LXR ligand on AT phagocytosis in RAW-LXRα macrophages. F) Efficacy of control, Mer-, ApoE- and ABCA1-specific siRNAs on protein expression in mouse primary peritoneal macrophages. G) Effect of control, Mer-, ApoE- and ABCA1-specific siRNAs on the ability of LXR agonists to promote AT uptake by primary macrophages. *P < 0.05; **P < 0.001.

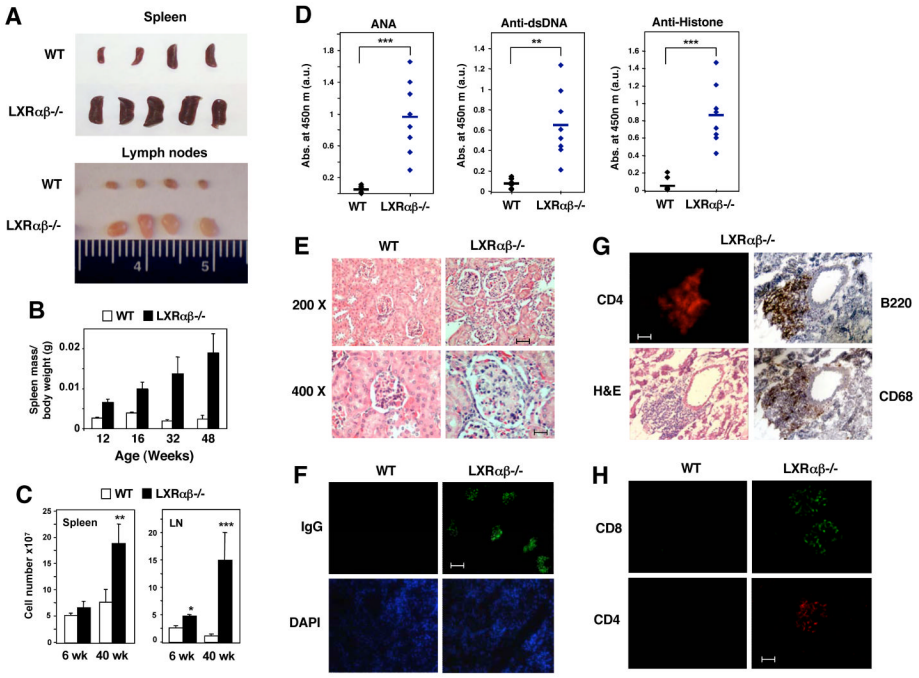

Figure 6. *Lxr*αβ-/- mice develop age-dependent autoimmune disease

A) Spleen and lymph nodes isolated from 40 week-old WT and *Lxr*αβ-/- mice. B) Analysis of spleen mass in WT and LXRαβ-/- mice. Spleens were isolated from WT and *Lxr*αβ-/- mice at the indicated age and spleen mass relative to body weight was measured. C) Total cell counts from spleen and lymph node of 40 week-old mice. D) 1:100 dilutions of serum samples obtained from 40 week-old WT (12 female mice) and *Lxr*αβ-/- mice (8 female mice) were analyzed for the presence of autoantibodies by ELISA. **P < 0.01, ***P < 0.001. E) Kidney sections (4 μm) from 40 week-old WT and *Lxr*αβ-/- female mice stained with H&E. F) Kidney sections from 40 week-old female mice stained with FITC-labeled anti-mouse IgG. Bar represents 50 μm. G) Consecutive kidney sections from 40 week-old female mice were stained with anti-mouse CD4**,** B220, CD68 and H&E. Bar represents 50 μm. H) Kidney sections from 40 week-old WT and LXRαβ-/- female mice stained with anti-CD8 and anti-CD4 antibodies. Bar represents 25 μm.

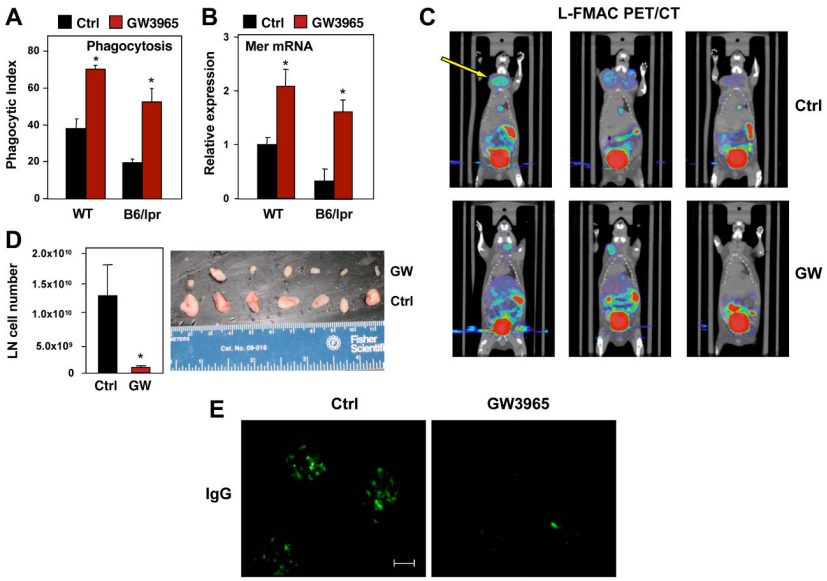

Figure 7. Treatment with an LXR agonist ameliorates autoimmune disease in mice

A) Peritoneal macrophages obtained from WT and B6$^{lpr/lpr}$ mice were treated with GW3965 for 24 h and phagocytosis was analyzed by confocal microscopy. B) Gene expression in macrophages from WT and B6$^{lpr/lpr}$ mice treated as in A. C) L-FMAC and PET/CT imaging of B6$^{lpr/lpr}$ mice. Images were analyzed using AMIDE software. *N* = 5/group; representative images are shown. D) Lymph node cellularity in 8-week old B6$^{lpr/lpr}$ female mice treated for 4 months with GW3965. *N* = 5/group. E). Representative kidney sections from female B6$^{lpr/lpr}$ mice treated with GW3965 for 4 months. Sections were analyzed by anti-immunoglobulin staining. Bar represents 50 μm. *N* = 6/group. Representative images are shown.